Diversification of the structural determinants of fibroblast growth factor-heparin interactions; implications for binding specificity

Ruoyan Xu[1], Alessandro Ori[1,2], Timothy R Rudd[1,3], Katarzyna A. Uniewicz[1,4], Yassir A. Ahmed[1], Scott E Guimond[1], Mark A Skidmore[1,5], Giuliano Siligardi[6], Edwin A Yates[1*] and David G Fernig[1*]

1. Institute of Integrative Biology, Department of Chemical and Structural Biology, University of Liverpool, Crown Street, Liverpool. L69 7ZB UK
2. Structural and Computational Biology Unit, European Molecular Biology Laboratory. 69117 Heidelberg, Germany
3. Istituto di Chimica e Biochmica, "G. Ronzoni", Via G. Colombo 81, Milano. 20133 Italy
4. PromoCell GmbH, Sickingenstr. 63/65, 69126 Heidelberg, Germany
5. Institute for Science and Technology in Medicine, Huxley Building, Keele University, Staffs. ST5 5BG UK
6. Diamond Light Source Ltd., Harwell Science and Innovation Campus, Didcot. OX11 0DE UK

*Equally contributing authors

Running title: Heparin binding sites of fibroblast growth factors

Corresponding authors: Professor DG. Fernig and Dr EA Yates, Department of Structural and Chemical Biology, Biosciences Building, Crown Street, University of Liverpool, Liverpool, L69 7ZB, UK. Tel. +44 (0)151 795 4471, Fax +44 (0)151 795 4406, Email: dgfernig@liverpool.ac.uk

SUPPLEMENTAL CONTENTS

SUPPLEMENTAL FIGURES

FIGURE S1 Optical biosensor analysis of the interaction of FGF-1 with DP8
The binding kinetics of FGF-1 to immobilized DP8 were measured, as described under "**Experimental procedures**". Different concentrations of FGF-1 were added to a streptavidin-derivatized amino silane cuvette functionalized with reducing end biotinylated DP8 (**Experimental procedures**). *A*, the association curves of the binding of different concentrations of FGF-1 were followed for one min. *B-F*, The distribution of the data points (jagged line) around a one-site model (horizontal line at 0 arc s) is shown for each of the concentrations of the FGF-1 used in the binding assay in panel A. Instrument noise is ± 0.5 arc s. Concentrations of FGF-1 are 85.9 nM (B), 60.1 nM (C), 45.8 nM (D), 22.9 nM (E) and 17.2 nM (F). *G*, Relationships between slope of initial rate, determined from a one-site binding model and concentration of FGF-1. *H*, relationships between k_{on}, determined from a one-site model and concentration of FGF-1.

Figure S1

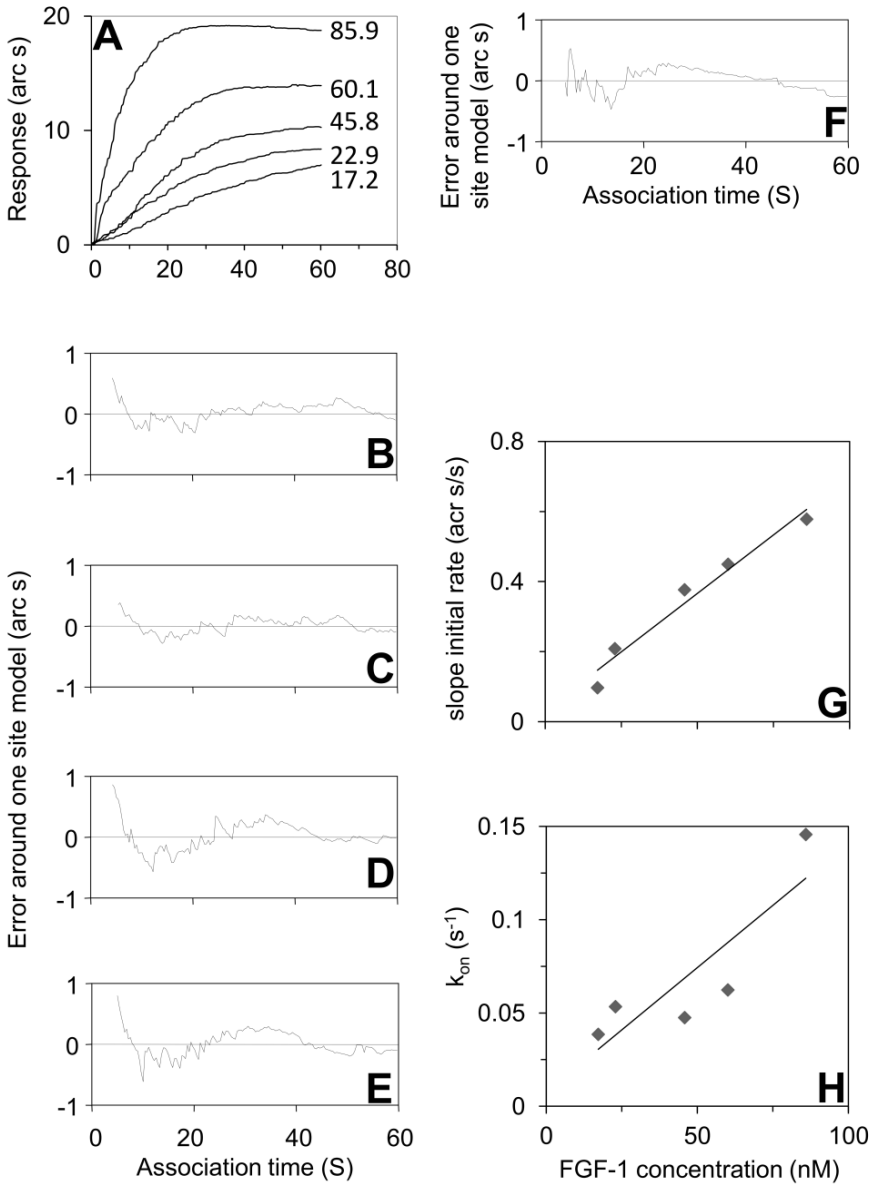

FIGURE S2 Optical biosensor analysis of the interaction of FGF-1 with DP8

The binding kinetics of FGF-1 to immobilized DP8 were measured, as described under "**Experimental procedures**". Different concentrations of FGF-1 were added to a streptavidin-derivatized amino silane cuvette functionalized with reducing end biotinylated DP8 (**Experimental procedures**). *A*, the association curves of the binding of different concentrations of FGF-1 were followed for one min. *B-F*, The distribution of the data points (jagged line) around a one-site model (horizontal line at 0 arc s) is shown for each of the concentrations of the FGF-1 used in the binding assay in panel A. Instrument noise is ± 0.5 arc s. Concentrations of FGF-1 are 22.8 nM (B), 20 nM (C), 17.1 nM (D), 14.3 nM (E), 11.4 nM (F) 8.6 nM (G) and 5.7 nM (H). *I*, Relationships between slope of initial rate, determined from a one-site binding model and concentration of FGF-1. *J*, relationships between k_{on}, determined from a one-site model and concentration of FGF-1.

Figure S2

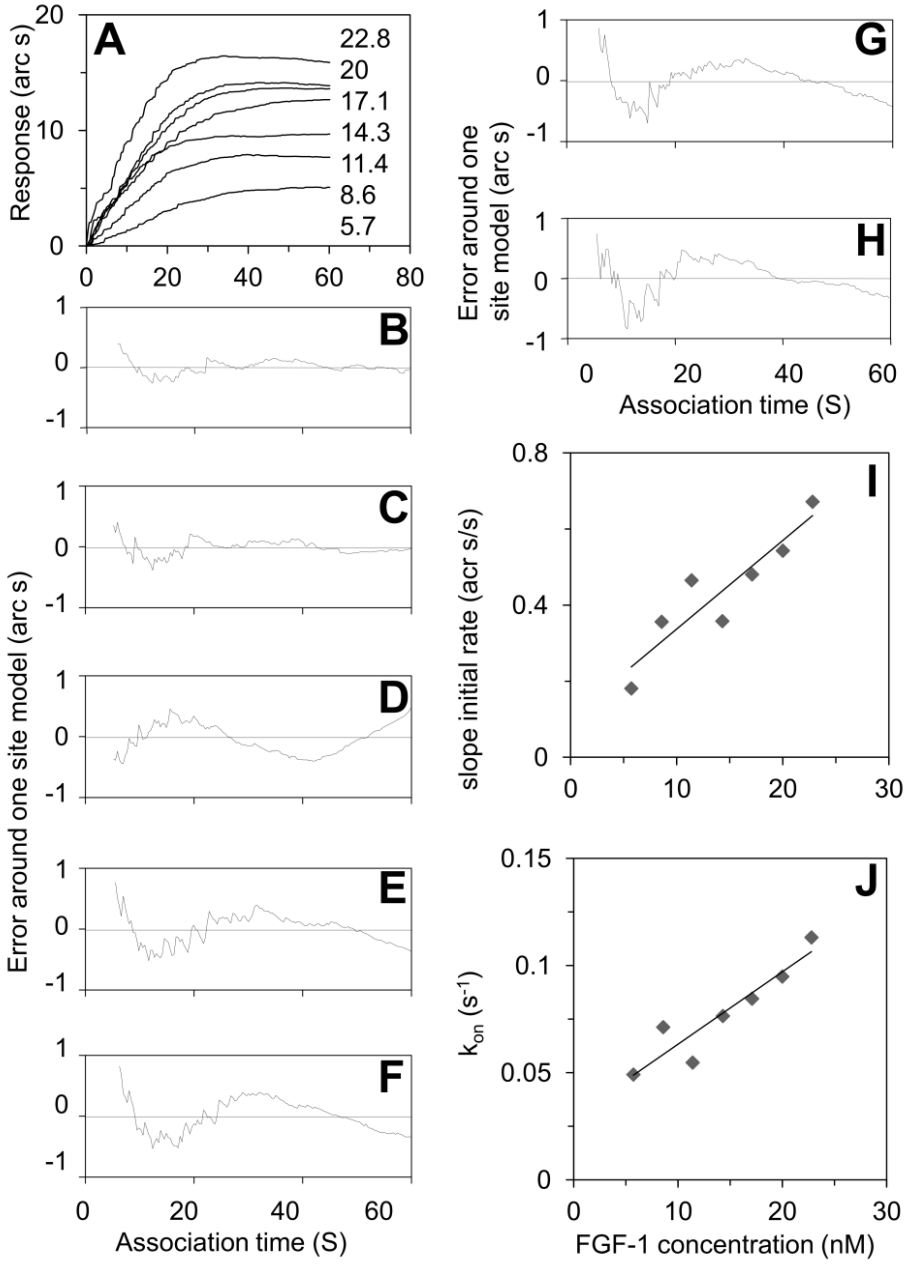

FIGURE S3 Optical biosensor analysis of the interaction of FGF-1 with DP8

The binding kinetics of FGF-1 to immobilized DP8 were measured, as described under "**Experimental procedures**". Different concentrations of FGF-1 were added to a streptavidin-derivatized amino silane cuvette functionalized with reducing end biotinylated DP8 (**Experimental procedures**). *A*, the association curves of the binding of different concentrations of FGF-1 were followed for one min. *B-F*, The distribution of the data points (jagged line) around a one-site model (horizontal line at 0 arc s) is shown for each of the concentrations of the FGF-1 used in the binding assay in panel A. Instrument noise is ± 0.5 arc s. Concentrations of FGF-1 are 22.8 nM (B), 20 nM (C), 14.3 nM (D), 11.4 nM (E), 8.6 nM (F) and 5.7 nM (G). *H*, Relationships between slope of initial rate, determined from a one-site binding model and concentration of FGF-1. *I*, relationships between k_{on}, determined from a one-site model and concentration of FGF-1.

Figure S3

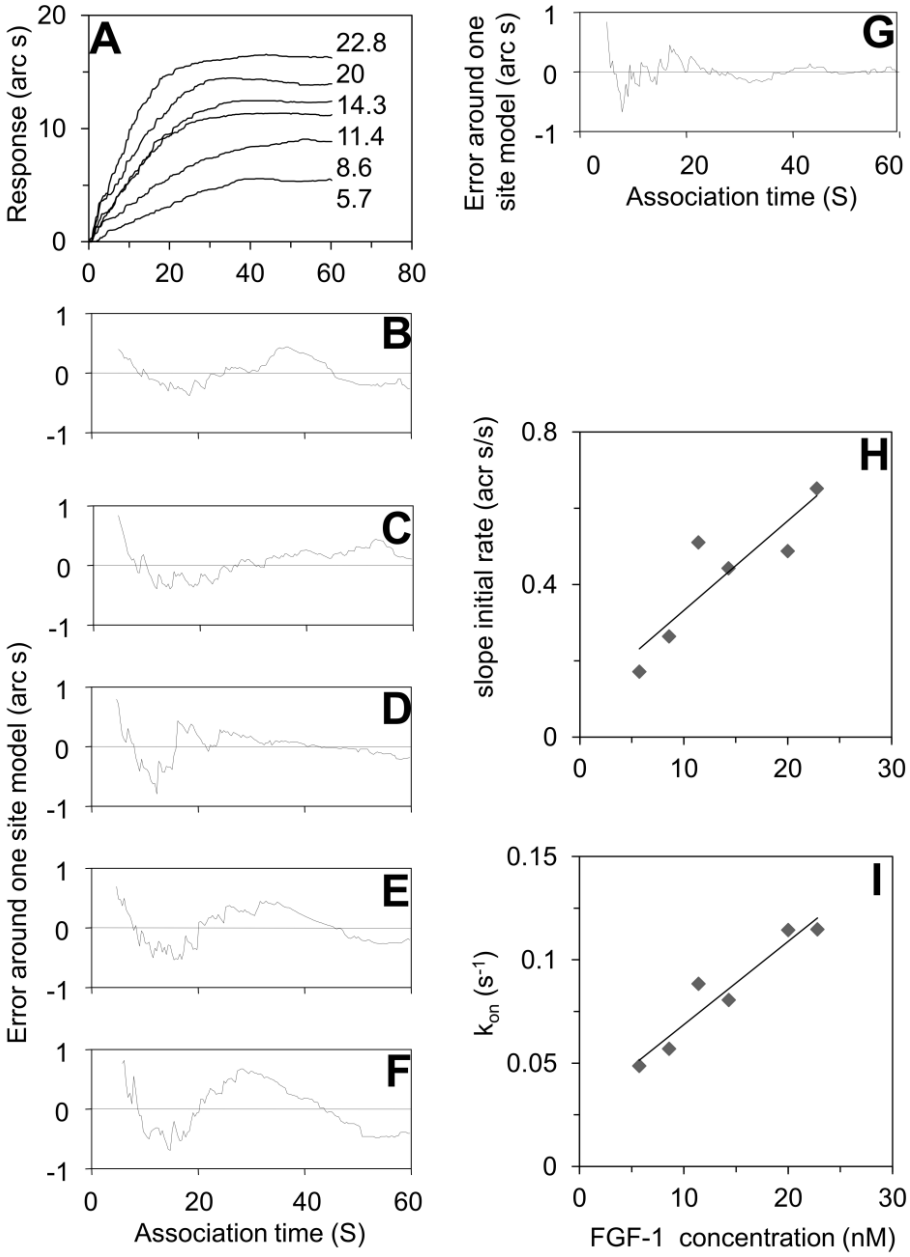

FIGURE S4 Optical biosensor analysis of the interaction of FGF-7 with DP8

The binding kinetics of FGF-7 to immobilized DP8 were measured, as described under "**Experimental procedures**". Different concentrations of FGF-7 were added to a streptavidin-derivatized amino silane cuvette functionalized with reducing end biotinylated DP8 (**Experimental procedures**). *A*, the association curves of the binding of different concentrations of FGF-7 were followed for one min. *B-F*, The distribution of the data points (jagged line) around a one-site model (horizontal line at 0 arc s) is shown for each of the concentrations of the FGF-7 used in the binding assay in panel A. Instrument noise is ± 0.5 arc s. Concentrations of FGF-7 are 190 nM (B), 106 nM (C), 95.2 nM (D), 47.6 nM (E), 23.8 nM (F) and 15.9 nM (G). *H*, Relationships between slope of initial rate, determined from a one-site binding model and concentration of FGF-7. *I*, relationships between k_{on}, determined from a one-site model and concentration of FGF-7.

Figure S4

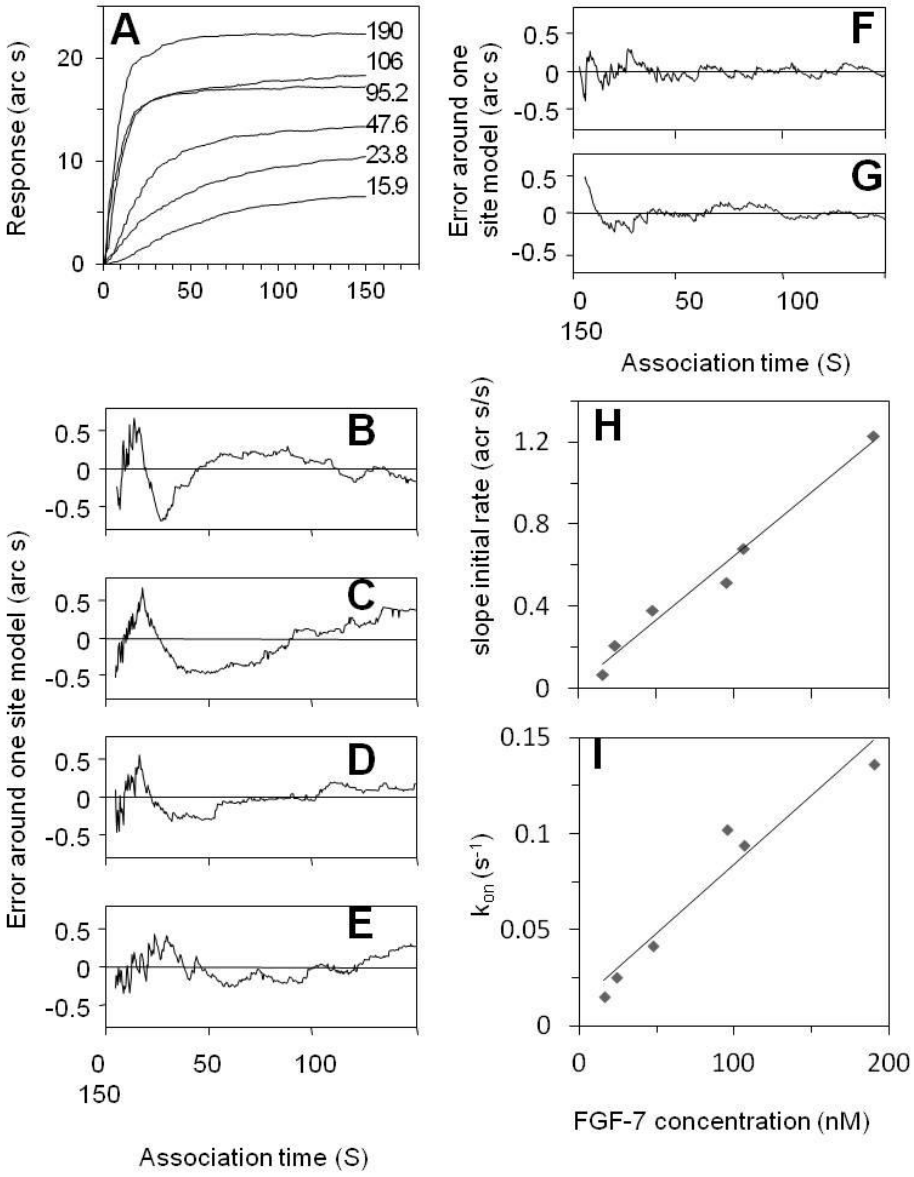

FIGURE S5 Optical biosensor analysis of the interaction of FGF-7 with DP8

The binding kinetics of FGF-7 to immobilized DP8 were measured, as described under "**Experimental procedures**". Different concentrations of FGF-7 were added to a streptavidin-derivatized amino silane cuvette functionalized with reducing end biotinylated DP8 (**Experimental procedures**). *A*, the association curves of the binding of different concentrations of FGF-7 were followed for one min. *B-F*, The distribution of the data points (jagged line) around a one-site model (horizontal line at 0 arc s) is shown for each of the concentrations of the FGF-7 used in the binding assay in panel A. Instrument noise is ± 0.5 arc s. Concentrations of FGF-7 are 212 nM (B), 105 nM (C), 79.5 nM (D), 47.7 nM (E), 31.8 nM (F) and 15.9 nM (G). *H*, Relationships between slope of initial rate, determined from a one-site binding model and concentration of FGF-7. *I*, relationships between k_{on}, determined from a one-site model and concentration of FGF-7.

Figure S5

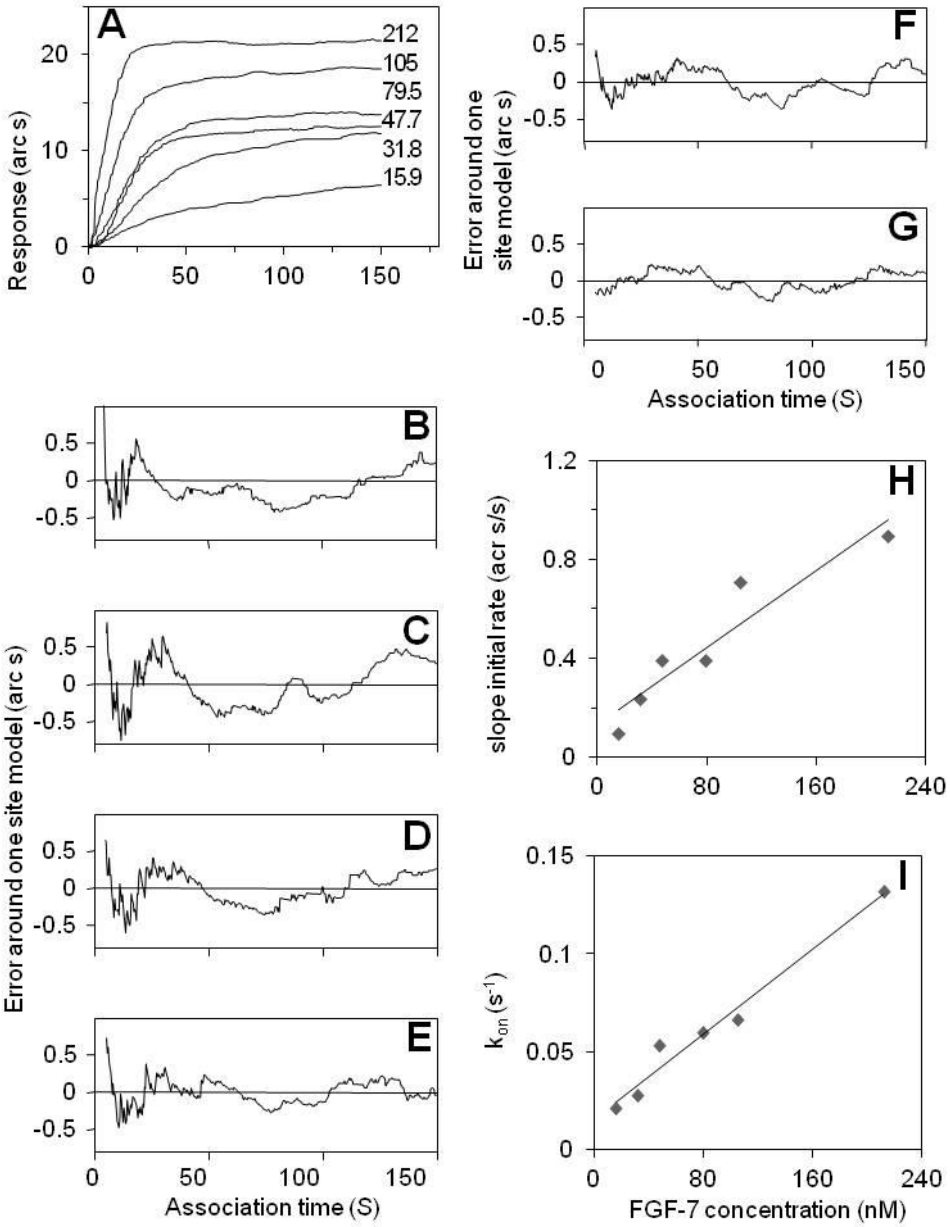

FIGURE S6 Optical biosensor analysis of the interaction of FGF-7 with DP8

The binding kinetics of FGF-7 to immobilized DP8 were measured, as described under "**Experimental procedures**". Different concentrations of FGF-7 were added to a streptavidin-derivatized amino silane cuvette functionalized with reducing end biotinylated DP8 (**Experimental procedures**). *A*, the association curves of the binding of different concentrations of FGF-7 were followed for one min. *B-F*, The distribution of the data points (jagged line) around a one-site model (horizontal line at 0 arc s) is shown for each of the concentrations of the FGF-7 used in the binding assay in panel A. Instrument noise is ± 0.5 arc s. Concentrations of FGF-7 are 106 nM (B), 79.4 nM (C), 47.7 nM (D), 23.8 nM (E) and 15.9 nM (F). *G*, Relationships between slope of initial rate, determined from a one-site binding model and concentration of FGF-7. *H*, relationships between k_{on}, determined from a one-site model and concentration of FGF-7.

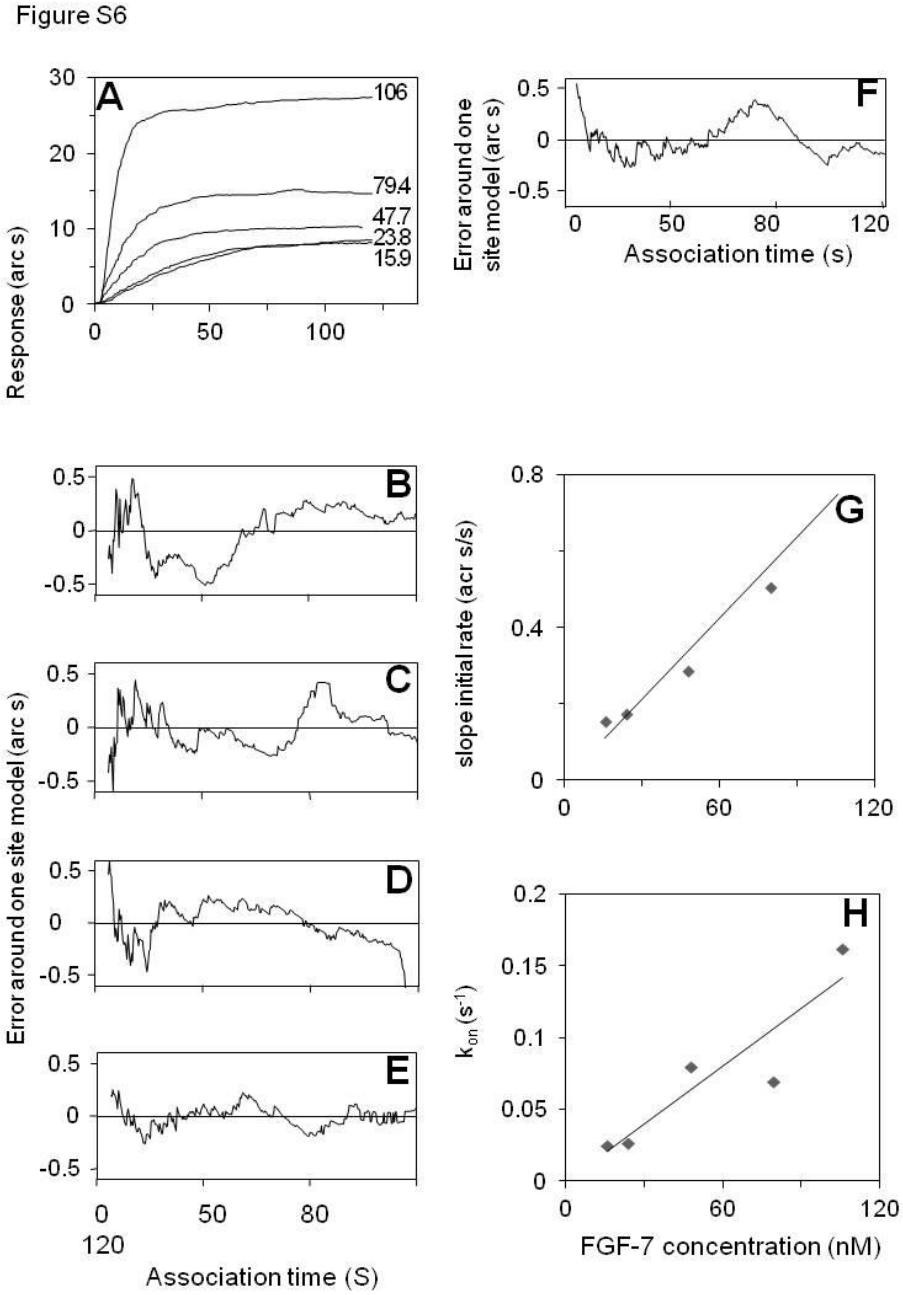

FIGURE S7 Optical biosensor analysis of the interaction of FGF-9 with DP8

The binding kinetics of FGF-9 to immobilized DP8 were measured, as described under "**Experimental procedures**". Different concentrations of FGF-9 were added to a streptavidin-derivatized amino silane cuvette functionalized with reducing end biotinylated DP8 (**Experimental procedures**). *A*, the association curves of the binding of different concentrations of FGF-9 were followed for one min. *B-F*, The distribution of the data points (jagged line) around a one-site model (horizontal line at 0 arc s) is shown for each of the concentrations of the FGF-9 used in the binding assay in panel A. Instrument noise is ± 0.5 arc s. Concentrations of FGF-9 are 169 nM (B), 152 nM (C), 102 nM (D), 76.2 nM (E) and 50.8 nM (F). *G*, Relationships between slope of initial rate, determined from a one-site binding model and concentration of FGF-9. *H*, relationships between k_{on}, determined from a one-site model and concentration of FGF-9.

Figure S7

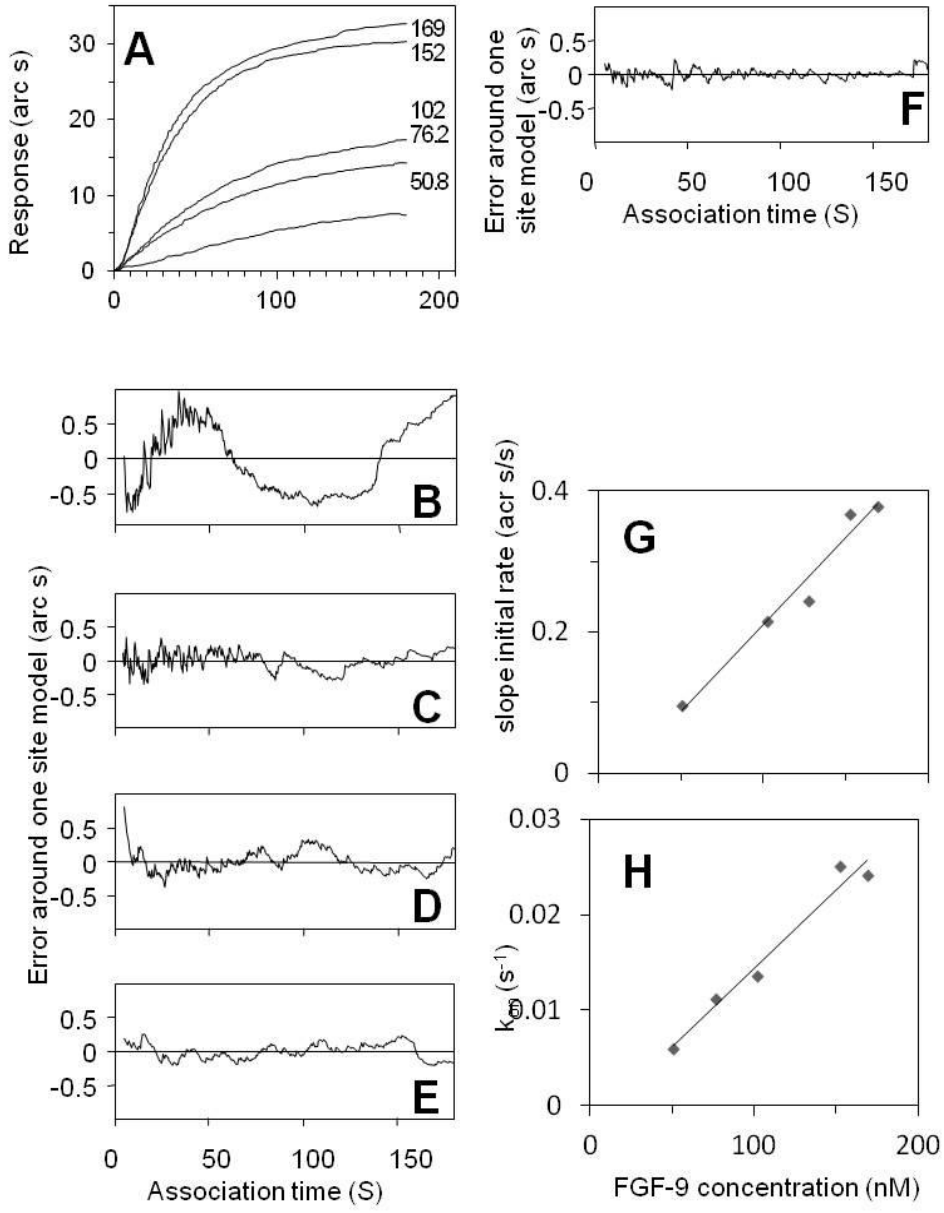

FIGURE S8 Optical biosensor analysis of the interaction of FGF-9 with DP8

The binding kinetics of FGF-9 to immobilized DP8 were measured, as described under "**Experimental procedures**". Different concentrations of FGF-9 were added to a streptavidin-derivatized amino silane cuvette functionalized with reducing end biotinylated DP8 (**Experimental procedures**). *A*, the association curves of the binding of different concentrations of FGF-9 were followed for one min. *B-F*, The distribution of the data points (jagged line) around a one-site model (horizontal line at 0 arc s) is shown for each of the concentrations of the FGF-9 used in the binding assay in panel A. Instrument noise is ± 0.5 arc s. Concentrations of FGF-9 are 169 nM (B), 152 nM (C), 127 nM (D), 102 nM (E), 76.2 nM (F) and 50.8 nM (G). *H*, Relationships between slope of initial rate, determined from a one-site binding model and concentration of FGF-9. *I*, relationships between k_{on}, determined from a one-site model and concentration of FGF-9.

Figure S8

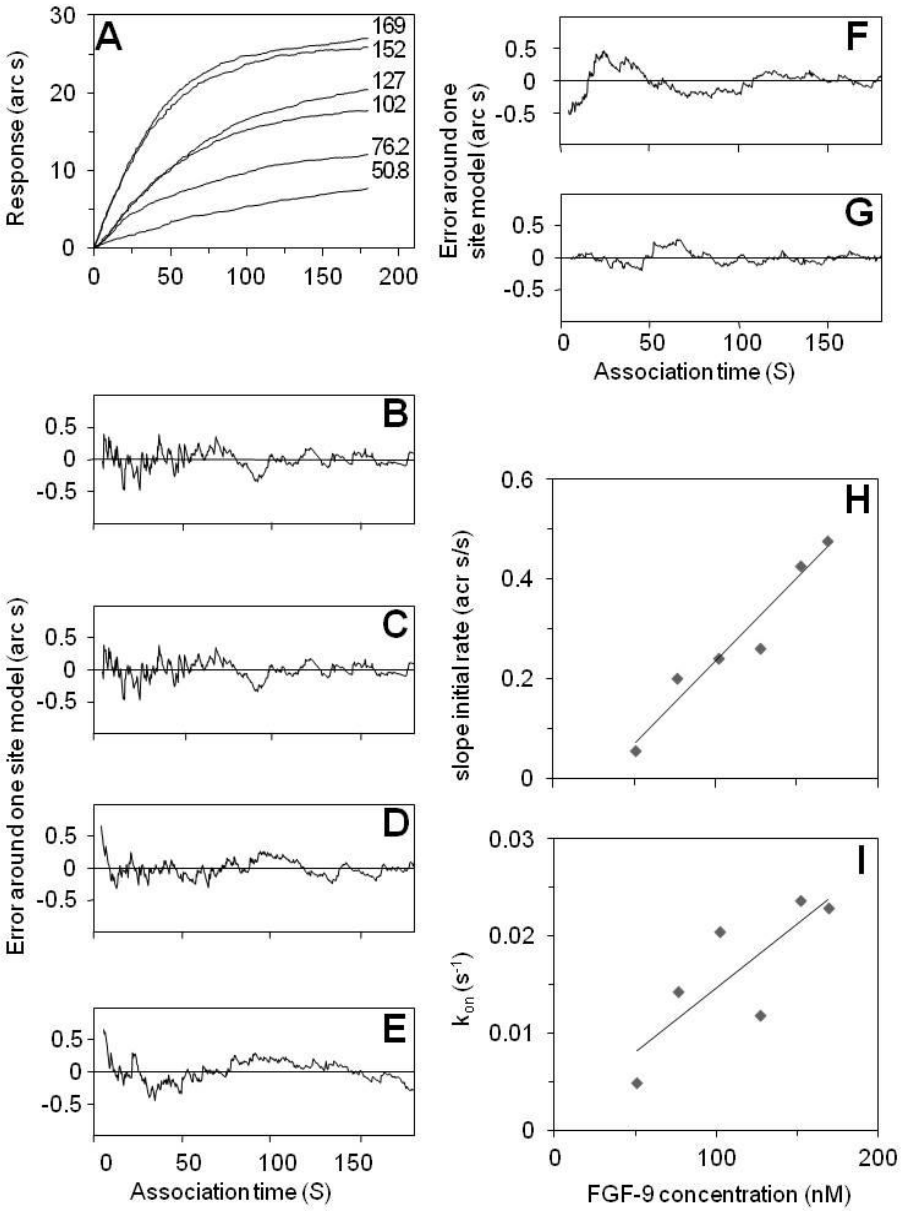

FIGURE S9 Optical biosensor analysis of the interaction of FGF-9 with DP8

The binding kinetics of FGF-9 to immobilized DP8 were measured, as described under "**Experimental procedures**". Different concentrations of FGF-9 were added to a streptavidin-derivatized amino silane cuvette functionalized with reducing end biotinylated DP8 (**Experimental procedures**). *A*, the association curves of the binding of different concentrations of FGF-9 were followed for one min. *B-F*, The distribution of the data points (jagged line) around a one-site model (horizontal line at 0 arc s) is shown for each of the concentrations of the FGF-9 used in the binding assay in panel A. Instrument noise is ± 0.5 arc s. Concentrations of FGF-9 are 169 nM (B), 152 nM (C), 127 nM (D), 102 nM (E) and 50.8 nM (F). *G*, Relationships between slope of initial rate, determined from a one-site binding model and concentration of FGF-9. *H*, relationships between k_{on}, determined from a one-site model and concentration of FGF-9.

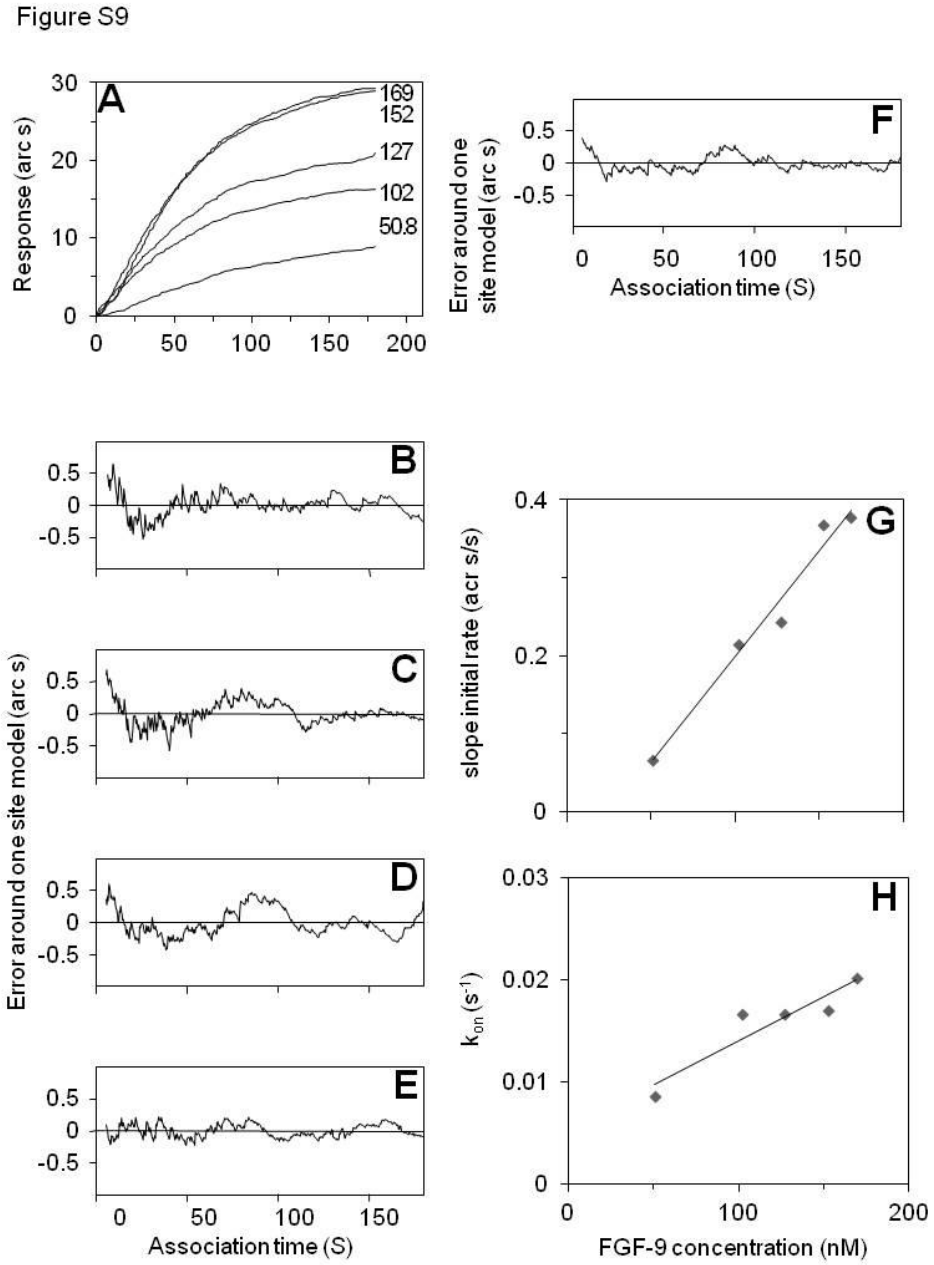

FIGURE S 10 Microscale Thermophoresis analysis of the interaction of FGF-18 with DP8
FGF-18 bound to a heparin column to protect lysine residues important for sugar binding was labeled with NT-647 dye (**Experimental procedures**). The concentration of the labeled protein was kept constant at low nM concentration, while the concentration of the unlabeled sugar was varied. The samples were loaded into hydrophilic MST-grade glass capillaries after a short incubation period and an MST-Analysis was performed using the Monolith NT.115 (**Experimental procedures**). The normalized fluorescence F_{norm} is plotted for different concentrations of DP8. *A* K_D value of 50 nM was determined for this interaction. *B.* K_D value of 26 nM was determined for this interaction.

Figure S10

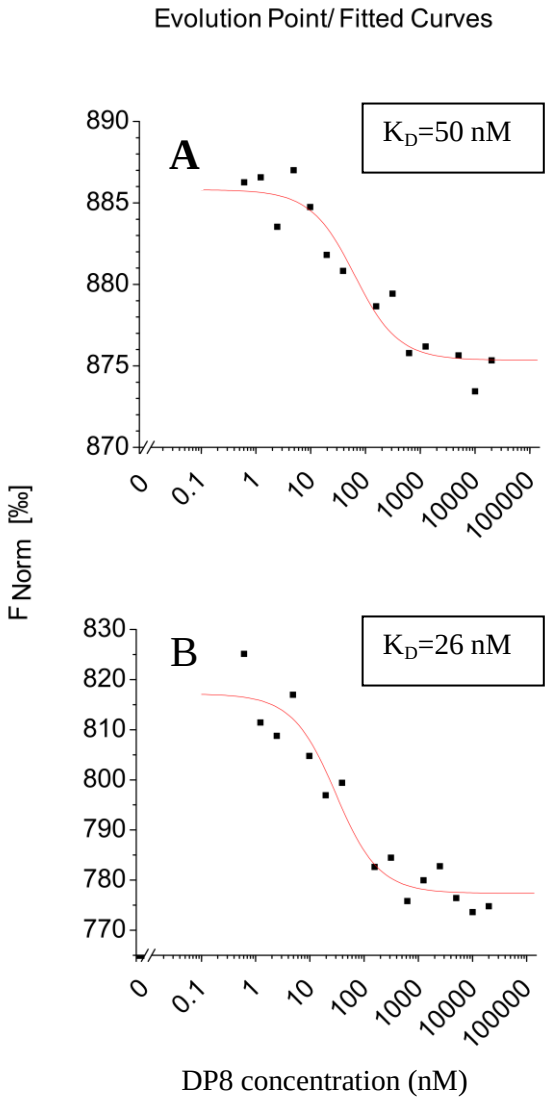

FIGURE S11. Differential scanning fluorimetry FGF-9 bound to heparin.
Differential scanning fluorimetry of 5 μM FGF-9 in the presence of different concentrations of heparin (**Experimental procedures**): *A.* Melting curve profiles of FGF-9 (5 μM) with a range of heparin concentrations (0 μM-25 μM). *B.* The first derivative of the melting curves in (A). *C.* Peak of the first derivative of the melting curves from (B), which is the melting temperature, T_m (mean of triplicates +/- SE).

Figure S11

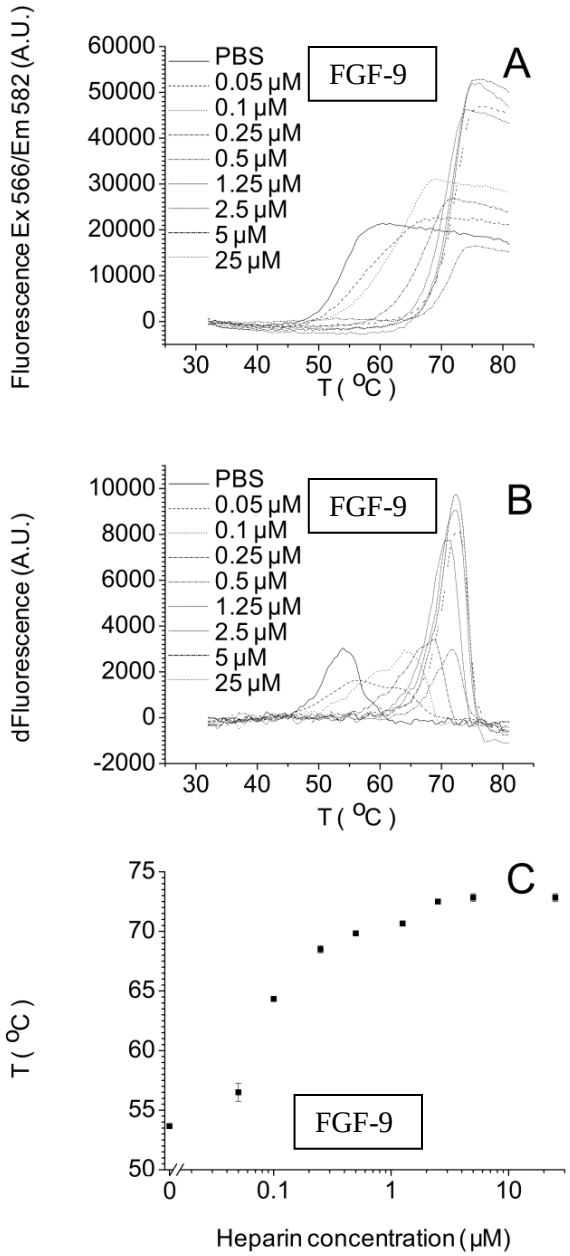

FIGURE S12. Differential scanning fluorimetry FGF-21 bound to heparin.

Differential scanning fluorimetry of 5 μM FGF-21 in the presence of different concentrations of heparin (**Experimental procedures**): *A.* Melting curve profiles of FGF-21 (5 μM) with a range of heparin concentrations (0 μM-500 μM). *B.* The first derivative of the melting curves in (A). *C.* Peak of the first derivative of the melting curves from (B), which is the melting temperature, T_m (mean of triplicates +/- SE).

Figure S12

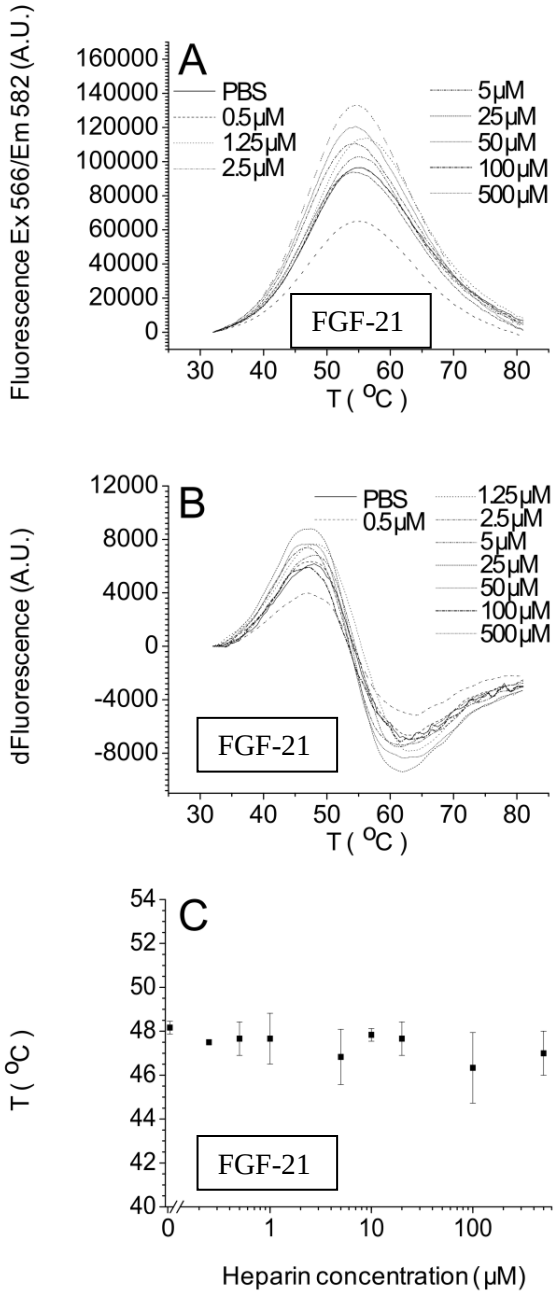

FIGURE S13. Differential scanning fluorimetry FGF-1, FGF-2 and FGF-18 binding to heparin derivatives.

Differential scanning fluorimetry was performed with a range of heparin-based poly- with 5 μM protein and 0.175 mg/mL sugar. The relative thermal stabilization effect of: Controls (PBS and heparin), Cation modified heparin forms and other GAGs (HS, HA, CS and DS). Results are the mean of triplicates after normalisation +/- SE, an apparent absence of error bar is due to a small SE).

Figure S13

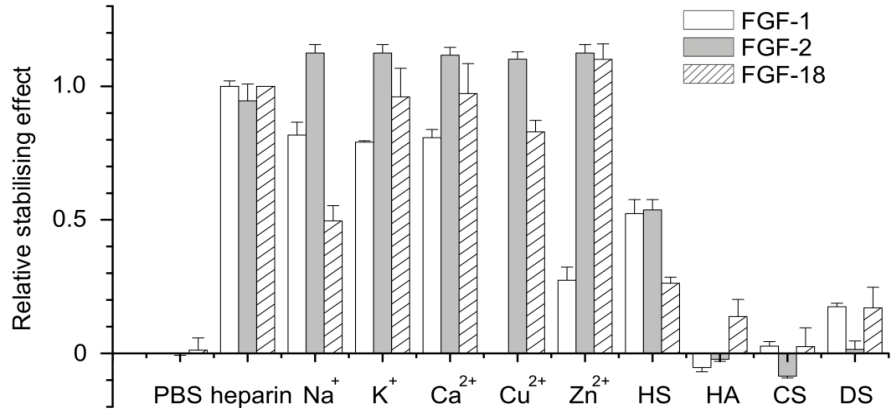

SUPPLEMENTAL TABLES

Table S1

Peptides identified by Protect and Label corresponding to the heparin binding sites of FGF-1, FGF-7, FGF-9 and FGF-18

The heparin binding sites were identified by Protect and Label (**Experimental procedures**) following purification the biotinylated peptides were identified by tandem mass spectrometry and analysed by Protein Prospector package v.5.9.2. The lists comprise the biotinylated peptides, with the site of biotinylation and any other modifications. According to this approach, the following ions can be considered as marker ions: m/z 84.08 and m/z 227.08 corresponding to Lys-NH_3 and biotin, m/z 310.16 assigned as Lys(biotin)-NH_3 and m/z 126.1 assigned as Lys(acetyl)-NH_3 (1).

Following tandem mass spectrometry of biotin labelled peptides, at least 10 of the most intense ions in each sample were fragmented by HCD and analyzed in the Orbitrap (Experimental Procedures). Data analysis included four chemical modifications: biotinylation, acetylation, carboxymethylation and oxidation.

In some cases, peptides possessed lysines that were only partly protected. Thus, they were both identified as acetyl and biotin derivatives, e.g., peptide of FGF-1, ^{113}-ISKKHAEKNWF-^{123} (**Table S1A**). This is likely to be caused by some of these lysines dissociating for sufficient time during the protection step to react with NHS-acetate, (The residues only labelled by biotin either remain bound or dissociate for too short a time to react in the protection step). When the site is univocally assigned the SLIP score is reported: e.g. Biotin@8=15 means that biotinylation on the lysine number 8 has a SLIP score of 15. As a rule of thumb a slip score >6 is ~ 95% confidence in site assignment.

[a.] m/z, mass(m)-over-charge(z) and it is the mass of the peptide divided by its charge. For MALDI charge is always +1, but for electrospray based mass spectrometry it is often +2 and +3.

[b.] z is the charge state of the peptide.

[c.] ppm, part per million, which indicates the error on the measurement of the precursor ion.

[d.] DB peptide is the peptide sequence.

[e.] Variable modification is the peptide modification: in some instances there is more than one combination of modifications that will yield an appropriate m/z with same probability. These are separated by the symbol "|". @ indicates the number of the modified residue and the number after = is a score for the assignment of the modification called SLIP score.

[f.] RT is retention time.

[g.] Score is the score assigned to the peptide identification by the search engine.

[h.] Expect is the probability associated with peptide identification (the lower the greater the likelihood of the assignment being correct).

Table S1 A

FGF-1: Uniprot Acc.: P05230, Uniprot ID: FGF1_HUMAN, Species: HUMAN, Name: Heparin-binding growth factor 1, Organism: Homo sapiens, Gene: FGF1, Protein MW: 17459.8 Protein pI: 6.5 Protein Length: 155

Sequence of human FGF-1, labeled peptides are colored in red.

1-80 MAEGEITTFTALTEKFNLPPGNYKKPKLLYCSNGGHFLRILPDGTVDGTRDRSDQHIQLQLSAESVGEVYIKSTETGQYL

81-155 AMDTDGLLYGSQTPNEECLFLERLEENHYNTYISKKHAEKNWFVGLKKNGSCKRGPRTHYGQKAILFLPLPVSSD

Peptides and their modifications identified by mass spectrometry

m/z[a]	z[b]	ppm[c]	DB Peptide[d]	Variable Mods[e]	RT[f]	Score[g]	Expect[h]
659.827	4	0.91	VGLKKNGSCKRGPRTHY	Biotin@4;Biotin@5;Carbamidomethyl@9;Biotin@10	3240	30.4	2.60E-09
818.405	3	0.64	VGLKKNGSCKRGPRTHY	Biotin@4=15;Acetyl@5=14;Carboxymethyl@9;Biotin@10=14	2805	16.5	6.30E-07
941.461	2	0.52	ISKKHAEKNWF	Biotin@8=34;Acetyl@3&Biotin@4|Acetyl@4&Biotin@3	5693	26.4	9.00E-07
552.618	3	1.6	ISKKHAEKNWF	Acetyl@3&Biotin@4|Acetyl@4&Biotin@3	3958	31.8	1.10E-06
879.76	3	-0.55	VGLKKNGSCKRGPRTHY	Biotin@4;Biotin@5;Carboxymethyl@9;Biotin@10	3356	17.9	1.10E-06
538.613	3	-0.024	ISKKHAEKNWF	Biotin@3|4	3044	26.7	2.10E-06
828.422	2	0.79	ISKKHAEKNWF	Biotin@8=15;Acetyl@3|4	4309	23.2	2.40E-06
846.921	2	0.29	ISKKHAEKNW	Biotin@8=24;Biotin@3|4	3273	22.1	2.70E-06
613.973	3	0.27	ISKKHAEKNWF	Biotin@3=23;Biotin@4=23	4541	23.4	5.40E-06
807.417	2	0.7	ISKKHAEKNWF	Biotin@8=17	3665	16.9	1.10E-05
683.34	2	0.48	IKSTETGQYL	Biotin@2	3895	21.3	1.30E-05
689.333	3	1.1	ISKKHAEKNWF	Biotin@3;Biotin@4;Biotin@8	5876	19.9	2.00E-05
754.888	2	0.097	ISKKHAEKNW	Biotin@3=6;Acetyl@4=6	2415	15.3	2.20E-05
552.617	3	0.23	ISKKHAEKNWF	Acetyl@8=8;Biotin@3|4	4117	21.6	2.40E-05
867.927	2	0.6	ISKKHAEKNW	Biotin@3=30;Biotin@4=26;Acetyl@8=26	4040	21.4	3.70E-05
552.617	3	0.45	ISKKHAEKNWF	Biotin@8=11;Acetyl@3|4	4308	20.6	4.00E-05
627.977	3	0.68	ISKKHAEKNWF	Biotin@8=13;Acetyl@3&Biotin@4|Acetyl@4&Biotin@3	5617	19.2	4.20E-05
774.887	2	0.41	ISKKHAEKN	Biotin@8=38;Acetyl@3&Biotin@4|Acetyl@4&Biotin@3	2432	18.1	4.80E-05
849.427	2	-0.27	ISKKHAEKNWF	Acetyl@8=16;Acetyl@3&Biotin@4|Acetyl@4&Biotin@3	5430	16.1	5.40E-05
959.96	2	0.53	ISKKHAEKNW	Biotin@3;Biotin@4;Biotin@8	4636	17.4	5.90E-05
775.893	2	-0.34	ISKKHAEKNW	Acetyl@8=23;Acetyl@3&Biotin@4|Acetyl@4&Biotin@3	3346	15.2	6.00E-05
775.893	2	-0.34	ISKKHAEKNW	Acetyl@3=18;Acetyl@4=19;Biotin@8=18	3497	16.3	7.10E-05
849.427	2	-0.27	ISKKHAEKNWF	Acetyl@3&4&Biotin@8|Acetyl@3&8&Biotin@4|Acetyl@4&8&Biotin@3	5177	18.4	7.70E-05
941.461	2	0.78	ISKKHAEKNWF	Biotin@3=21;Biotin@4=18;Acetyl@8=18	5505	17.8	8.70E-05
849.428	2	0.59	ISKKHAEKNWF	Acetyl@3&4&Biotin@8|Acetyl@3&8&Biotin@4|Acetyl@4&8&Biotin@3	5012	18.9	1.30E-04
428.242	2	0.37	GQKAIL	Biotin@3	4366	16.6	1.80E-04
610.849	2	0.3	KKPKLL	Biotin@4=17;Acetyl@1&Biotin@2|Acetyl@2&Biotin@1	5831	16.9	1.90E-04
518.815	2	-0.22	KKPKLL	Acetyl@1=12;Acetyl@2=11;Biotin@4=11	5182	18.5	4.10E-04
610.849	2	0.5	KKPKLL	Acetyl@1&Biotin@2&4|Acetyl@2&Biotin@1&4|Acetyl@4&Biotin@1&2	5682	16.6	4.30E-04
867.927	2	0.46	ISKKHAEKNW	Biotin@8=16;Acetyl@3&Biotin@4|Acetyl@4&Biotin@3	4195	15.9	5.90E-04
518.815	2	0.48	KKPKLL	Acetyl@4=12;Acetyl@1&Biotin@2|Acetyl@2&Biotin@1	5031	17.9	7.20E-04
600.346	2	-0.17	KKPKLLY	Acetyl@1&2&Biotin@4|Acetyl@1&4&Biotin@2|Acetyl@2&4&Biotin@1	5443	16.7	9.30E-04

Table S1B

Peptides identified by Protect and Label which corresponded to FGF-7 heparin binding sites

Uniprot Acc.: P21781 Uniprot ID: FGF7_HUMAN Species: HUMAN Name: Keratinocyte growth factor, Organism: Homo sapiens Gene: FGF7,

Protein MW: 22509.4 Protein pI: 9.3 Protein Length: 194

Sequence of human FGF-7, labeled peptides are colored in red.

1-80 MHKWILTWILPTLLYRSCFHIICLVGTISLACNDMTPEQMATNVNCSSPERHTRSYDYMEGGDIRVRRLFCRTQWYLRID
81-160 KRGKVKGTQEMKNNYNIMEIRTVAVGIVAIKGVESEFYLAMNKEGKLYAKKECNEDCNFKELILENHYNTYASAKWTHNG
161-194 GEMFVALNQKGIPVRGKKTKKEQKTAHFLPMAIT

Peptides and their modifications identified by mass spectrometry

m/z[a]	z[b]	ppm[c]	DB Peptide[d]	Variable Mods[e]	RT[f]	Score[g]	Expect[h]
665.5878	4	1.1	RIDKRGKVKGTQEMKNNY	Biotin@9=9;Acetyl@15=23;Biotin@4|7	4914	19.1	2.60E-04
722.1085	4	2.8	RIDKRGKVKGTQEMKNNY	Biotin@4=36;Biotin@7=32;Biotin@9=19;Acetyl@15=19	6479	17.2	2.90E-04
744.7269	3	1.5	YLRIDKRGKVKGTQEM	Acetyl@11=21;Acetyl@6&Biotin@9|Acetyl@9&Biotin@6	6128	19.2	3.20E-04
725.8576	2	0.72	LAMNKEGKLY	Oxidation@3;Biotin@5=10;Acetyl@8=10	6385	18	4.50E-04
1232.3158	3	3.3	VALNQKGIPVRGKKTKKEQ KTAHF	Biotin@6=7;Biotin@17=9;Acetyl@20=9;Acetyl@13&Biotin@14&16 |Acetyl@14&Biotin@13&16|Acetyl@16&Biotin@13&14	8016	16.1	4.80E-04
1137.9135	3	-1.5	NQKGIPVRGKKTKKEQKTA HF	Biotin@3=13;Biotin@14=9;Acetyl@17=9;Acety l@10&Biotin@11&13|Acetyl@11&Biotin@10&13|Acetyl@13&Biotin@10&11	7426	17	4.90E-04
807.6741	4	3.3	NQKGIPVRGKKTKKEQKTA HF	Acetyl@17=18;Acetyl@3&14&Biotin@10&11&13|Acetyl@10&11&Biotin@3&13&14| Acetyl@10&13&Biotin@3&11&14|Acetyl@10&14&Biotin@3&11&13	6999	15.9	7.40E-04
831.3652	2	1.9	ASAKWTHNGGEMF	Biotin@4	7114	15.1	8.90E-04
821.9487	4	-0.88	VALNQKGIPVRGKKTKKEQ KTAHF	Biotin@6=17;Acetyl@13&14&16&Biotin@17|Acetyl@13&14&16&Biotin@20|Acetyl@13&14&17 &Biotin@16|Ace tyl@13&14&20&Biotin@16|Acetyl@13&14&20&Biotin@17|Acetyl@13&16&17 &Biotin@14|Ace tyl@13&16&20&Biotin@14|Acetyl@13&17&20&Biotin@14|Acetyl@13&16&20 &Biotin@17|Acetyl@13&17&20&Biotin@16|Acetyl@14&16&17&Biotin@13|Acetyl@14&16&20 &Biotin@13|Acety l@14&17&20& Biotin@13|Acetyl@16&17&20&Biotin@13|Acetyl@14&16&20 &Biotin@17|Acetyl@14&17&20&Biotin@16|Acetyl@16&17&20&Biotin@14	6426	15.9	9.80E-04

Table S1 C

Peptides identified by Protect and Label which corresponded to FGF-9 heparin binding sites

Uniprot Acc.: P31371, Uniprot ID: FGF9_HUMAN, Species: HUMAN, Name: Glia-activating factor, Organism: Homo sapiens, Gene: FGF9, Protein MW: 23440.7, Protein pI: 7.1, Protein Length: 208

Sequence of human FGF-9, labeled peptides are colored in red.

1-80 MAPLGEVGNYFGVQDAVPFGNVPVLPVDSPVLLSDHLGQSEAGGLPRGPAVTDLDHLKGILRRRQLYCRTGFHLEIFPNG
81-160 TIQGTRKDHSRFGILEFISIAVGLVSIRGVDSGLYLGMNEKGELYGSEKLTQECVFREQFEENWYNTYSSNLYKHVDTGR
161-208 RYYVALNKDGTPREGTRTKRHQKFTHFLPRPVDPDKVPELYKDILSQS

Peptides and their modifications identified by mass spectrometry

m/z[a]	z[b]	ppm[c]	DB Peptide[d]	Variable Mods[e]	RT[f]	Score[g]	Expect[h]
1039.863	3	2.9	VALNKDGTPREGTRTKRHQKF	Biotin@5;Biotin@16;Biotin@20	5895	22.1	5.10E-06
516.6642	5	-0.66	HLEIFPNGTIQGTRKDHSRF	Biotin@15	6836	17.1	1.10E-04
1125.074	2	-0.72	THFLPRPVDPDKVPELY	Biotin@12	8652	19.3	1.60E-04
453.2316	3	0.65	KHVDTGRRY	Biotin@1	2709	21.1	4.60E-04

Table S1 D

Peptides identified by Protect and Label which corresponded to FGF-18 heparin binding sites

Uniprot Acc.: O76093, Uniprot ID: FGF18_HUMAN, Species: HUMAN, Name: Fibroblast growth factor 18, Organism: Homo sapiens, Gene: FGF18, Protein MW: 23988.9, Protein pI: 9.9, Protein Length: 207

Sequence of human FGF-18, labeled peptides are colored in red.

1-80 MYSAPSACTCLCLHFLLLCFQVQVLVAEENVDFRIHVENQTRARDDVSRKQLRLYQLYSRTSGKHIQVLGRRISARGEDG

81-160 DKYAQLLVETDTFGSQVRIKGKETEFYLCMNRKGKLVGKPDGTSKECVFIEKVLENNYTALMSAKYSGWYVGFTKKGRPR

161-207 KGPKTRENQQDVHFMKRYPKGQPELQKPFKYTTVTKRSRRIRPTHPA

Peptides and their modifications identified by mass spectrometry

m/z[a]	z[b]	ppm[c]	DB Peptide[d]	Variable Mods[e]	RT[f]	Score[g]	Expect[h]
1263.1241	2	3.4	MKRYPKGQPELQKPF	Biotin@2;Biotin@6;Biotin@13	8177	30.6	2.30E-06
723.3748	3	-2.1	KRYPKGQPELQKPF	Biotin@1=10;Biotin@12=42	6829	34.7	3.70E-06
767.057	3	0.7	MKRYPKGQPELQKPF	Biotin@6=10;Biotin@13=47	7328	29.6	8.90E-06
781.0624	3	3.1	MKRYPKGQPELQKPF	Biotin@2=10;Acetyl@6=10;Biotin@13=42	8007	29.6	1.20E-05
1197.6047	2	4.3	KRYPKGQPELQKPF	Biotin@1;Biotin@5;Biotin@12	8118	26.5	1.20E-05
705.7014	3	0.87	MKRYPKGQPELQKPF	Acetyl@6=10;Biotin@13=38	6717	30.6	1.20E-05
737.3826	3	3.8	KRYPKGQPELQKPF	Biotin@1=11;Acetyl@5=11;Biotin@12=37	7797	28.6	1.40E-05
676.025	3	1.3	KRYPKGQPELQKPF	Acetyl@1=51;Acetyl@5=39;Biotin@12=39	7377	24.3	1.50E-05
1013.5351	2	2.5	KRYPKGQPELQKPF	Biotin@1=8;Acetyl@5=8;Acetyl@12=50	7047	28.5	1.60E-05
662.0231	3	3.7	KRYPKGQPELQKPF	Acetyl@5=8;Biotin@12=36	6467	32.8	2.00E-05
737.3812	3	1.9	KRYPKGQPELQKPF	Biotin@12=38;Acetyl@1&Biotin@5|Acetyl@5&Biotin@1	7947	26.5	2.80E-05
662.0191	3	-2.3	KRYPKGQPELQKPF	Acetyl@12=25;Biotin@1|5	5994	26.6	3.00E-05
1058.0505	2	2.8	MKRYPKGQPELQKPF	Biotin@6=6;Acetyl@13=34	6433	29.6	3.10E-05
834.0881	3	-0.47	RKGKLVGKPDGTSKECVF	Biotin@2=30;Biotin@4=20;Acetyl@14=21;Carbamidomethyl@16	6697	23.3	4.10E-05
786.3913	3	-0.41	MKRYPKGQPELQKPF	Oxidation@1;Biotin@2=45;Biotin@6=25;Acetyl@13=25	7250	21.5	4.50E-05
1105.5688	2	2.4	KRYPKGQPELQKPF	Biotin@1=46;Biotin@5=27;Acetyl@12=27	7579	18.2	5.00E-05
767.0577	3	1.6	MKRYPKGQPELQKPF	Biotin@2=13;Biotin@13=31	7021	20.2	5.60E-05
705.7009	3	0.16	MKRYPKGQPELQKPF	Biotin@2=10;Acetyl@13=34	6261	30.7	5.60E-05
781.0605	3	0.66	MKRYPKGQPELQKPF	Biotin@2=41;Biotin@6=31;Acetyl@13=31	7837	26.6	6.20E-05
992.5297	2	2.4	KRYPKGQPELQKPF	Acetyl@12=29;Biotin@1|5	6177	29.5	6.60E-05
719.7047	3	0.55	MKRYPKGQPELQKPF	Biotin@2=10;Acetyl@6=10;Acetyl@13=44	7327	26.6	7.90E-05
873.9468	2	1.1	GSQVRIKGKETEF	Acetyl@7=10;Biotin@9=10	6398	20.2	9.20E-05
637.3211	3	0.57	GSQVRIKGKETEFY	Acetyl@7=16;Biotin@9=16	6807	15	9.20E-05
676.0225	3	-2.4	KRYPKGQPELQKPF	Acetyl@1=10;Biotin@5=10;Acetyl@12=27	7228	22.3	9.40E-05
1044.4918	3	5.8	CMNRKGKLVGKPDGTSKECVF	Carbamidomethyl@1;Biotin@5=38;Biotin@7=26;Carbamidomethyl@19;Acetyl@11&Biotin@17|Acetyl@17&Biotin@11	8173	17.2	1.20E-04
1084.5636	2	2.6	KRYPKGQPELQKPF	Biotin@12=36;Biotin@1|5	6997	23.4	1.20E-04
969.1294	3	3	CMNRKGKLVGKPDGTSKECVF	Carbamidomethyl@1;Biotin@5=30;Biotin@7=19;Carbamidomethyl@19;Acetyl@11|17	6936	18.3	1.30E-04
1030.4867	3	4.4	CMNRKGKLVGKPDGTSKECVF	Carbamidomethyl@1;Biotin@5=28;Biotin@7=19;Biotin@17=9;Carbamidomethyl@19	7476	20.3	1.60E-04
872.1047	3	2.2	NRKGKLVGKPDGTSKECVF	Biotin@3=22;Biotin@5=15;Acetyl@15=15;Carbamidomethyl@17	6674	25.5	1.70E-04
933.4596	3	1.2	NRKGKLVGKPDGTSKECVF	Biotin@3=22;Biotin@5=15;Biotin@15=13;Carbamidomethyl@17	7258	26.5	1.70E-04
648.0171	3	-0.0012	KRYPKGQPELQKPF	Biotin@5=10	4899	22.3	1.90E-04
873.9473	2	1.7	GSQVRIKGKETEF	Biotin@7=19;Acetyl@9=19	6247	20.2	2.00E-04

1047.5133	2	2.2	GSQVRIKGKETEFY	Biotin@7;Biotin@9	7577	18.2	2.00E-04
662.0212	3	0.87	KRYPKGQPELQKPF	Biotin@1=12;Acetyl@5=12	5745	16.6	2.30E-04
786.3911	3	-0.66	MKRYPKGQPELQKPF	Oxidation@1;Biotin@2=20;Acetyl@6=20;Biotin@13=20	7798	19.1	2.60E-04
772.3875	3	-0.78	MKRYPKGQPELQKPF	Oxidation@1;Biotin@2=8;Biotin@13=16	6518	20.2	2.70E-04
637.3204	3	-0.53	GSQVRIKGKETEFY	Biotin@7=22;Acetyl@9=22	6662	16.1	2.70E-04
661.0129	3	1.5	GSQVRIKGKETEFYL	Biotin@7=13	7100	16.8	2.90E-04
729.8461	2	0.86	CMNRKGKL	Carbamidomethyl@1;Biotin@5;Biotin@7	5697	17	2.90E-04
648.0168	3	-0.46	KRYPKGQPELQKPF	Biotin@12=22	5560	31.7	3.90E-04
807.9112	2	1.3	MKRYPKGQPEL	Biotin@2=11;Acetyl@6=11	5603	16.3	4.00E-04
723.3759	3	-0.55	KRYPKGQPELQKPF	Biotin@1=19;Biotin@5=6	6369	16	4.00E-04
623.318	3	1.3	GSQVRIKGKETEFY	Biotin@7=19	5397	17.2	4.20E-04
909.4492	3	1.7	RKGKLVGKPDGTSKECVF	Biotin@2=27;Biotin@4=17;Carbamidomethyl@16;Acetyl@8&Biotin@14|Acetyl@14&Biotin@8	8150	17.2	4.50E-04
637.5895	4	1.6	RIHVENQTRARDDVSRKQL	Biotin@17	3617	16	5.10E-04
890.4363	4	2.1	TKKGRPRKGPKTRENQQDVHFM	Biotin@2;Biotin@3;Biotin@8;Biotin@11;Oxidation@22	5111	15.6	5.10E-04
694.3553	2	1.9	LCMNRKGKL	Carbamidomethyl@2;Acetyl@6=14;Biotin@8=14	5578	18	5.40E-04
623.3184	3	1.9	GSQVRIKGKETEFY	Biotin@9=11	5557	17.2	5.80E-04
786.3855	2	-2.5	LCMNRKGKL	Carbamidomethyl@2;Biotin@6;Biotin@8	6533	18	6.80E-04
602.6298	3	2.1	GRRISARGEDGDKY	Biotin@13	2508	17.3	7.50E-04
965.9811	2	1.8	GSQVRIKGKETEF	Biotin@7;Biotin@9	7249	16.1	7.80E-04
1008.8216	3	3.9	NRKGKLVGKPDGTSKECVF	Biotin@3;Biotin@5;Biotin@9;Biotin@15;Carbamidomethyl@17	8217	15	8.30E-04
834.4233	2	-0.18	KRYPKGQPEL	Biotin@1;Biotin@5	6052	15.4	8.90E-04
736.3723	3	1.6	GSQVRIKGKETEFYL	Biotin@7;Biotin@9	8278	16.1	8.90E-04
852.9408	2	0.33	GSQVRIKGKETEF	Biotin@9=10	5067	17.2	9.00E-04

Table S2

Comparison of the secondary structures FGFs deduced from SRCD spectra.

Sample	Helix1	Helix2	Strand1	Strand2	Turns	Unordered	Total
FGF-1	-0.001	0.027	0.293	0.195	0.228	0.250	0.993
5:1 (H:FGF-1)	0.053	0.083	0.211	0.111	0.211	0.339	1.009
FGF-2	0.000	0.018	0.247	0.118	0.297	0.314	0.994
5:1 (H:FGF-2)	0.000	0.000	0.015	0.096	0.285	0.610	1.006
FGF-7	0.211	0.136	0.043	0.067	0.231	0.314	1.001
5:1 (H:FGF-7)	0.001	0.000	0.012	0.094	0.284	0.608	0.999
FGF-9	0.536	0.224	0.001	0.001	0.107	0.139	1.008
5:1 (H:FGF-9)	0.054	0.082	0.210	0.110	0.211	0.337	1.004
FGF-18	0.000	0.000	0.015	0.095	0.285	0.609	1.004
5:1 (H:FGF-18)	0.054	0.083	0.211	0.110	0.212	0.335	1.004
FGF-21	0.421	0.245	0.050	0.038	0.117	0.137	1.008
5:1 (H:FGF-21)	0.422	0.245	0.050	0.038	0.117	0.138	1.009

SRCD spectra were recorded on beamline B-23 at Diamond Synchrotron between 180 nm and 260 nm of the FGF alone and in the presence of a 5-fold molar excess of heparin. The spectra were analysed by programmes Selcon 3 and Database 3 (**Experimental procedures**).

Table S3

FGF-7 and heparin complexes' concentrations and their mean TM values based on 3 repeats (± SE).

Heparin concentration		Molar ratio (heparin: FGF-7)	TM	
μg/mL	μM	-	°C	+/-
0	0	0	60.7	0.3
8.75	0.5	0.1	61	0
21.9	1.25	0.25	65.7	0.8
43.8	2.5	0.5	66.2	0.6
87.5	5	1	68.2	0.3
437.5	25	5	68	0.5
875	50	10	67.8	0.3
1750	100	20	68	0.5
8750	500	100	67.8	0.3

Table S4

FGF-9 and heparin complexes' concentrations and their mean TM values based on 3 repeats (± SE).

Heparin concentration		Molar ratio (heparin: FGF-9)	TM	
μg/mL	μM	-	°C	+/-
0	0	0	53.7	0.3
0.88	0.05	0.01	56.5	1.3
1.75	0.1	0.02	64.3	0.3
4.38	0.25	0.05	68.5	0.5
8.75	0.5	0.1	69.8	0.3
21.9	1.25	0.25	70.7	0.3
43.8	2.5	0.5	72.5	0
87.5	5	1	72.8	0.6
437.5	25	5	72.8	0.6

Table S5

FGF-21 and heparin complexes' concentrations and their mean TM values based on 3 repeats (± SE).

Heparin concentration		Molar ratio (heparin: FGF-21)	TM	
μg/mL	μM	-	°C	+/-
0	0	0	48.2	0.3
8.75	0.5	0.1	47.5	0
21.9	1.25	0.25	47.7	0.8
43.8	2.5	0.5	47.7	1.2
87.5	5	1	46.8	1.3
437.5	25	5	47.8	0.3
875	50	10	47.7	0.8
1750	100	20	46.3	1.6
8750	500	100	47	1.0

REFERENCE:

1. Ori, A., Free, P., Courty, J., Wilkinson, M.C., and Fernig, D.G. (2009) Identification of heparin-binding sites in proteins by selective labeling. *Mol. Cell Proteomics* **8**, 2256-2265